SEPARATIONS: MATERIALS, DEVICES AND PROCESSES



Anisotropic membrane materials for gas separations

Juan-Manuel Restrepo-Flórez¹ | Martin Maldovan^{1,2} |

¹School of Chemical & Biomolecular Engineering, Georgia Institute of Technology, Atlanta, Georgia

²School of Physics, Georgia Institute of Technology, Atlanta, Georgia

Correspondence

Martin Maldovan, School of Chemical & Biomolecular Engineering and School of Physics, Georgia Institute of Technology, Atlanta, GA 30332.

Email: maldovan@gatech.edu

Funding information

National Science Foundation, Grant/Award Number: 1744212

Abstract

To date the design of membranes for gas separations has relied on isotropic materials that control the magnitude of mass flux. However, mass flux is a vector quantity and controlling its direction is essential for complete manipulation of diffusion processes. In this article, we show how anisotropic materials enable control of mass flux direction in membranes and allow for novel mechanisms for gas separation. We present a detailed study of the design parameters that control membrane selectivities and permeances and demonstrate that this new class of membranes can provide a new avenue to obtain significant improvements with respect to isotropic materials. We also discuss how the proposed anisotropic membranes can be constructed using isotropic materials. Mass diffusion principles for gas separations in anisotropic membranes are different from those in isotropic materials and this novel strategy for the design of membranes can open new opportunities in membrane separation processes.

KEYWORDS

anisotropic mass transfer, gas separation, polymeric membranes

1 | INTRODUCTION

Separations in the chemical industry are responsible for 10-15% of the total world energy consumption and the emission of more than 100 million tons of CO₂ per year in the United States.¹ This high energy demand is due to the predominance of energy-intensive separation processes such as distillation and drying which require phase change. A more efficient alternative for separation is the use of membranes where the energy demand can be an order of magnitude lower than distillation.^{1,2} In the case of gas separations, the ability of membranes to selectively permeate gases has been studied for more than a century. However, the use of membranes in commercial applications has started nearly 40 years ago.³⁻⁵ The gradual advancement from scientific discovery to fully developed technologies can be partially explained by the lack of materials and fabrication processes that can produce membranes with large efficiencies. 4,5 Despite the success of membranes in the separation of gas mixtures such as N₂/O₂, CO₂/CH₄, H₂/CO, and N₂/Ar, widespread use of membranes is still far from reaching several important systems such as CO₂/N₂, CO₂/H₂, and Olefin/paraffin.^{3,4,6} Challenges hindering the use of membranes in new separation processes include efficiency, stability, and processability.^{3,4,7–10} In particular, being able to improve membrane efficiency is one of the challenges that has received significant attention in recent years, with several works aimed at designing membrane materials that simultaneously maximize selectivity and permeability.^{8–12}

The first generation of membranes for gas separations can be characterized by the use of homogeneous and isotropic materials. ^{7,8} These membranes have been widely used in gas separation processes due to their ease of fabrication and material availability. Membranes made of homogeneous isotropic materials have spatially-independent scalar diffusion coefficients. ^{11,13} Depending on their structural properties, homogeneous isotropic membranes for gas separations can be divided into dense membranes and molecular sieves. Dense membranes are comprised of flexible polymers (rubbery and glassy) or semi-rigid polymers (such as polymers of intrinsic micro porosity PIM and thermally rearranged polymers). ¹¹ In polymer membranes, chemical modifications to the polymer material can result in changes in polymer backbone mobility, chemical affinity for the different gases, and/or packing efficiency. All these physical properties provide an avenue to manipulate the solubility and diffusivity of the gas species

in the polymer. The ultimate goal is to establish the relation between chemical functionalization and the resultant transport properties such that permeabilities can be chemically tuned.^{7,8} On the other hand, in molecular sieves such as zeolites, metal organic frameworks, and carbon molecular sieves, the transport of gas is governed by the size of the nanopores in the sieve. In these nanoporous membranes, chemical functionalization is used to control the nanopore dimensions with the aim of tuning the membrane permeability.^{11,14-16} Despite of the wide use of homogeneous isotropic membranes for gas separations, flexible and semi-rigid polymers present limitations in terms of trade-off relations between selectivity and permeability, while molecular sieves often require difficult manufacturing processes.¹⁷

The second generation of membranes can be characterized by the use of nonhomogeneous materials. These membranes have recently been developed with the aim of partially overcoming the limitations of homogeneous membranes. 18-20 In this case, two or more materials are combined to yield an effective isotropic composite material with tailored transport properties and separation efficiencies. Ideally, the resultant composite material should have the advantages of its constituents and none of its limitations. 17 In nonhomogeneous isotropic membranes, the diffusion coefficient is spatially dependent and effective medium approaches are generally used to predict the effective properties of the membrane. 11,18 One type of nonhomogeneous membranes, known as mixed matrix membranes (MMM), consists of molecular sieves dispersed in a polymer matrix (either flexible or semirigid). MMM are expected to have high selectivity and permeability as the molecular sieves and be easily processed as the polymer matrix. In practice, however, challenging issues associated with polymer-sieve interactions often limit their performance. 18,20-22 The effective membrane permeability is typically calculated by using Maxwell's effective medium formulation. ¹⁸ Another type of nonhomogeneous membranes consists of connecting in series two materials whose performances are in the upper bound of a Robeson plot. In this case, the resulting composite bilayer membrane has improved permeability relative to the material with the lowest permeability and similar selectivity relative to the material with the highest selectivity. 19

To date most research efforts for membrane gas separation have been focused on isotropic membrane materials. In these materials, mass transfer occurs isotropically meaning that it is difficult to guide mass flow paths in controlled ways. Recent progress in mass diffusion metamaterials, however, has begun to create unprecedented ways to manipulate the direction of mass flux.²³⁻²⁸ A membrane that manipulates mass flux direction can control the trajectory of the compounds of interest and create spatial areas where the flux of the desired molecule is focused, or alternatively spatial areas where undesirable molecules are prevented from penetrating. Importantly, the rerouting of molecules to different locations provides a new physical principle that can be exploited to design gas separations. Such directional control of mass flux can be achieved in practice by means of engineered anisotropic membrane materials. ^{23,28} In practice, fabrication of these anisotropic membrane materials involves the use of layered arrangements of isotropic materials. Despite their unique potential, the design,

operation, capabilities, and limitations of anisotropic membrane materials to achieve gas separations are still largely unexplored.

In this article, we demonstrate novel anisotropic membranes that show significant performance improvements for gas separations. We reroute mass diffusion by engineering the local anisotropy of the membrane in order to guide molecules to specific areas. We also address some fundamental design questions associated with anisotropic membranes. For example, which structure geometries can be used and how are they operated to take advantage of flux directional control? What are the governing variables determining the performance of these membranes? And how these variables affect the performance and structure requirements for gas separation? The predictions and insights in this work pave the way for a new generation of membranes where mass diffusion and separation efficiencies are controlled by means of locally anisotropic materials.

2 | RESULTS AND DISCUSSION

We first present the theoretical and analytical approach that allows designing and enhancing the performance of separation processes using anisotropic membranes. Since separation principles in anisotropic systems are different from those in typical isotropic systems, rationally designed geometries (different from isotropic membranes) need to be considered in the anisotropic case. Specifically, in separation processes using isotropic membranes, separation occurs due to the different flux magnitudes for compounds crossing the membrane and a single permeate develops across the membrane. Flat sheets and hollow fibers are examples of membrane geometries generally used in separation processes involving isotropic materials.⁵ In contrast, in the separation processes considered here using anisotropic membranes, both magnitude and direction of mass flux are manipulated and separation occurs due to the different spatial rerouting of molecules A and B (Figure 1). In this case, two permeates develop with compositions that are functions of the position on the permeate side. As a result, when designing anisotropic membranes one has to define the region where the permeate is collected (e.g., Permeate 1 or Permeate 2) in order to take advantage of the rerouting of molecules trajectories. The basic role of the anisotropic shell is to manipulate the flux directions such that separation efficiency is maximized either for Permeate 1 or Permeate 2. Thus, in the anisotropic case, it is necessary to design new membrane geometries and operational strategies in order to collect the permeate fraction of interest. In our membrane designs, we consider the collection of the permeate from the core region (i.e., Permeate 1 in Figure 1). The membrane composite consists of a half-cylindrical core region surrounded by a cylindrical shell. The core (c) region ($r < R_1$) is made of an isotropic material with diffusivity $D_{c(i)}$ and solubility $S_{c(i)}$ for compound i, whereas the cylindrical shell (sh) $(R_1 < r < R_2)$ consists of an anisotropic material with diffusivity $D_{sh(i)\theta}$ in the azimuthal direction, diffusivity $D_{sh(i)r}$ in the radial direction, and solubility $S_{sh(i)}$. Permeation across the membrane develops due to a chemical potential driving force, where a constant partial pressure p_i is applied at $r = R_2$ and complete sweeping $p_i = 0$ is imposed at $-R_2 < x < R_2$, y = 0

FIGURE 1 Schematic of the proposed anisotropic membranes. The core region is isotropic while the surrounding shell is anisotropic. The role of the shell is to reroute compounds *A* and *B* through the membrane. The driving force is the chemical potential difference at the top and bottom of the membrane. Separation of *A* from *B* is obtained for permeate 1 leaving the core. A schematic of a prototype module design is shown on the right where independent collection channels are used for the two generated permeate streams

for all compounds leaving the system. At the interface between the core and the shell $(r=R_1)$, flux continuity in the radial direction is enforced and the partition coefficient $K_{(i)} = S_{c(i)}/S_{sh(i)}$ is used to account for concentration discontinuities due to changes in solubilities. By considering Fick's law $J_{(i)} = -\overline{\overline{D}}_{(i)} \nabla C_{(i)}$ and continuity equations, the concentration distribution for species i in the anisotropic membrane is given by the Fourier series expansions²⁸:

$$C_{c(i)}(r,\theta) = \sum_{n=1}^{\infty} a_{n(i)} r^n \sin(n\theta)$$
 (1)

$$C_{sh(i)}(r,\theta) = \sum_{n=1}^{\infty} \left[b_{n(i)} r^{nl_{(i)}} + c_{n(i)} r^{-nl_{(i)}} \right] \sin(n\theta)$$
 (2)

where $l_{(i)}^2 = D_{sh(i)\theta}/D_{sh(i)r}$. By applying the boundary conditions, we find that the series coefficients can be written as

$$a_{n(i)} = p_{(i)} S_{sh(i)} \frac{4}{\pi} \left[\frac{1 - (-1)^n}{n} \right] K_{(i)} \theta_{n(i)} R_1^{-n}$$
(3)

$$b_{n(i)} = p_{(i)} S_{sh(i)} \frac{2}{\pi} \left[\frac{1 - (-1)^n}{n} \right] (1 + \delta_{(i)}) \theta_{n(i)} R_1^{-nl_{(i)}}$$
(4)

$$c_{n(i)} = p_{(i)} S_{sh(i)} \frac{2}{\pi} \left[\frac{1 - (-1)^n}{n} \right] (1 - \delta_{(i)}) \theta_{n(i)} R_1^{nl_{(i)}}$$
 (5)

$$\theta_{n(i)} = \left[\left(1 + \delta_{(i)} \right) \left(\frac{R_2}{R_1} \right)^{n I_{(i)}} + \left(1 - \delta_{(i)} \right) \left(\frac{R_2}{R_1} \right)^{-n I_{(i)}} \right]^{-1} \tag{6}$$

where $\delta_{(i)} = D_{c(i)} S_{c(i)} / \sqrt{D_{sh(i)\theta}} D_{sh(i)r} S_{sh(i)}$. Using this analytical solution, we calculate the average fluxes $\langle J_{(i)y} \rangle$ for compound i leaving the core along the y-direction (Permeate 1) and obtain analytical expressions for normalized permeance (Equation (7)) and ideal selectivity (Equation (8)) of the anisotropic membrane.

$$\frac{P_{(i)}}{P_{(i)}^*} = \left(\frac{1}{P_{(i)}^*}\right) \frac{\langle J_{(i)y} \rangle}{\Delta p_{(i)}} = \frac{4}{\pi} \sum_{n=1}^{\infty} \left[\frac{1 - (-1)^n}{n}\right] \theta_{n(i)}$$
 (7)

$$\frac{\alpha_{A/B}}{\alpha_{A/B}^*} = \frac{\sum_{n=1}^{\infty} \left[\frac{1 - (-1)^n}{n} \right] \theta_{n(A)}}{\sum_{n=1}^{\infty} \left[\frac{1 - (-1)^n}{n} \right] \theta_{n(B)}}$$
(8)

where $P_{(i)}^* = D_{c(i)}S_{c(i)}/R_1$ is the isotropic core permeance and $\alpha_{A/B}^* = \frac{D_{c(A)}S_{c(B)}}{D_{c(B)}S_{c(B)}}$ is the isotropic core selectivity. Note that $P_{(i)}/P_{(i)}^*$ and $\alpha_{A/B}/\alpha_{A/B}^*$ measure the changes in permeance and selectivity due to the anisotropic shell with respect to the permeance and selectivity of the core.

It is interesting to note that a small number of nondimensional variables is required to characterize the membrane in terms of normalized selectivities and permeances [Equations 7-8]. In particular, for the separation of two gases A and B, the variables are: R_2/R_1 , $I_{(A)}$, $I_{(B)}$, $\delta_{(A)}$, and $\delta_{(B)}$. That is $\alpha_{A/B}/\alpha_{A/B}^* = f(R_2/R_1, I_{(A)}, I_{(B)}, \delta_{(A)}, \delta_{(B)})$ and $P_{(i)}/P_{(i)}^* =$ $g(R_2/R_1, I_{(i)}, \delta_{(i)})$. The first nondimensional variable R_2/R_1 is geometrical and represents the relative thickness of the shell. The variable $\delta_{(i)}$ is the ratio between the core material intrinsic permeability (i.e., $D_{c(i)}S_{c(i)}$) and the intrinsic permeability of the anisotropic material (i.e., $\sqrt{D_{sh(i)\theta}D_{sh(i)r}}S_{sh(i)}$). In addition, $I_{(A)}$ and $I_{(B)}$ are nondimensional variables that characterize the anisotropicity of the shell. The variables $I_{(A)}$ and $I_{(B)}$ are of special interest because they determine the specific anisotropic mass diffusion of A and B induced by the shell. We show in Figure 2 (left panels) the preferred trajectories of A and B for different values of $I_{(A)}$ and $I_{(B)}$ when a binary mixture is diffusing through the anisotropic membranes. Note that when $I_{(i)} > 1$ (i = A, B), we have $D_{sh(i)\theta} > D_{sh(i)r}$ and the anisotropic shell causes compound i to mainly detour around the core, whereas for $I_{(i)}$ < 1, we have $D_{sh(i)\theta}$ < $D_{sh(i)r}$ and the shell causes compound i to mainly focus toward the core. Therefore, depending on the values of $I_{(A)}$ and $I_{(B)}$ there exist four different scenarios. The membrane can (a) focus molecules of A toward the core and shield molecules of B from the core $(I_{(A)} < 1, I_{(B)} > 1;$ Figure 2a), (b) detour both A and B around the core $(I_{(A)} > 1, I_{(B)} > 1;$ Figure 2b), (c) focus both A and B ($I_{(A)}$ < 1, $I_{(B)}$ < 1; Figure 2c), and (d) shield A and focus B ($I_{(A)} > 1$, $I_{(B)} < 1$; Figure 2d). Note that most materials used in membrane science and technology are isotropic and lie at the origin of the plot (i.e., $I_{(i)} = 1$, and $D_{sh(i)\theta} = D_{sh(i)r}$).

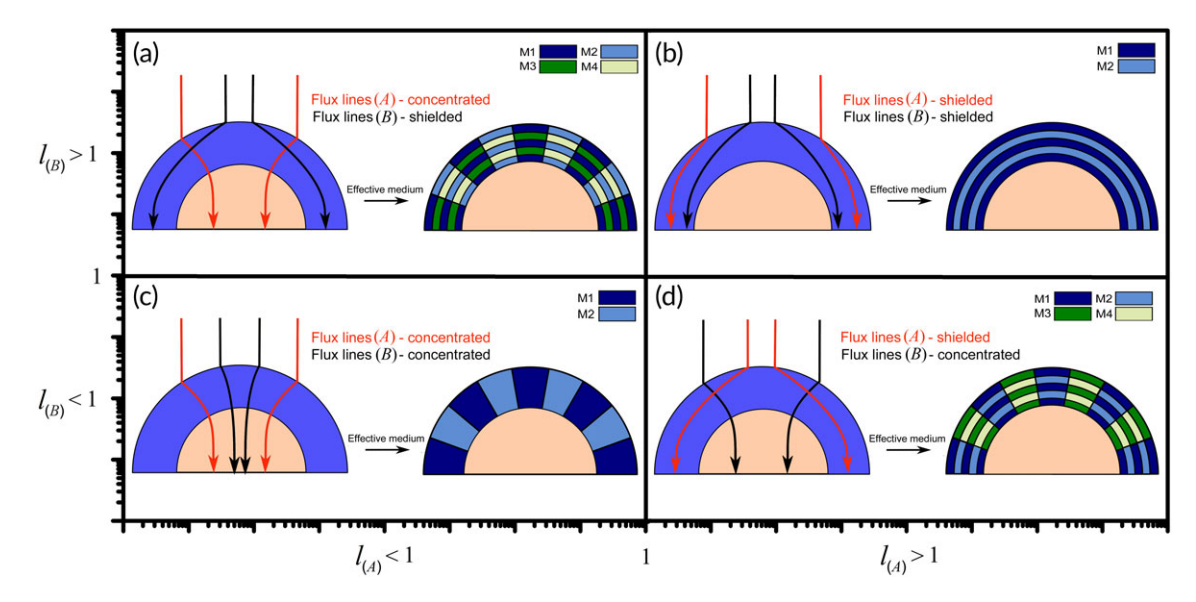


FIGURE 2 Schematic for the effect of the anisotropic shell on the trajectory of compounds A and B (a) $I_A < 1$, $I_B > 1$ (b) $I_A > 1$, $I_B > 1$ (c) $I_A < 1$, $I_B < 1$ (d) $I_A > 1$, $I_B < 1$. The shell structures made of isotropic materials that can create such mass diffusion trajectories are shown on the right

We also show in Figure 2 (right panels) the corresponding shell structures that provide the anisotropic properties required to obtain the mass diffusion trajectories for A and B. We note that the shell structures are made of homogeneous and isotropic materials. The anisotropic structures made of isotropic materials are designed by using effective medium theory.²⁹⁻³¹ For example, to obtain $l_{(0)} > 1$ (i.e., $D_{sh(i)\theta} > D_{sh(i)r}$), a multilayer shell made of alternating materials M_1 and M2 aligned along the azimuthal direction provides the required anisotropic shell structure where compound i prefers the azimuthal direction for diffusion (Figure 2b).²⁹ In this case, the azimuthal diffusivity $D_{sh(i)\theta}$ of the shell is given by a parallel diffusion model (Equation 9) while the radial diffusivity $D_{sh(i)r}$ is given by a series model (Equation 10). The diffusivities $D_{1(i)}$ and $D_{2(i)}$ and solubilities $S_{1(i)}$ and $S_{2(i)}$ of the constitutive materials M_1 and M_2 that yield the anisotropic structure with properties $D_{sh(i)r}$, $D_{sh(i)\theta}$, and $S_{sh(i)}$, can be found by solving the effective medium equations

$$D_{sh(i)}^{Parallel} = \frac{1}{\left(f_1 + f_2 k_i^*\right)} \left(f_1 D_{1(i)} + f_2 k_i^* D_{2(i)}\right) \tag{9}$$

$$\frac{1}{D_{\text{sh(i)}}^{\text{Series}}} = \left(f_1 + f_2 k_i^*\right) \left(\frac{f_1}{D_{1(i)}} + \frac{f_2}{k_i^* D_{2(i)}}\right) \tag{10}$$

$$S_{sh(i)} = f_1 S_{1(i)} + f_2 S_{2(i)}, \quad k_i^* = \frac{S_{2(i)}}{S_{1(i)}}$$
 (11)

where f_1 and f_2 are the volume fractions of materials M_1 and M_2 and $k_{(i)}^*$ is the partition coefficient for compound i between materials M_1 and M_2 . Analogously, to obtain $I_{(i)} < 1$ (i.e., $D_{sh(i)\theta} < D_{sh(i)r}$) a multilayer shell made of materials M_1 and M_2 aligned along the radial direction (i.e., in series in the azimuthal direction and in parallel in the radial direction) provides the anisotropic shell structure where the radial

direction is preferred for diffusion (Figure 2c). To obtain $I_{(A)} < 1$, $I_{(B)} > 1$ (Figure 2a) or $I_{(A)} > 1$, $I_{(B)} < 1$ (Figure 2d) different structural arrangements are required. In the first case, compound A should effectively see shell layers aligned along the radial direction $(D_{sh(A)\theta} < D_{sh(A)\theta})$ while compound B should see shell layers along the azimuthal direction $(D_{sh(B)\theta} > D_{sh(B)r})$, (and vice versa for the second case). The required shell material properties for compounds A and B can be obtained simultaneously by arranging four materials M_1 , M_2 , M_3 , and M_4 as shown in Figure 2a,d. The properties of these materials must be selected such that for $I_{(A)} < 1$, $I_{(B)} > 1$

while for $I_{(A)} > 1$, $I_{(B)} < 1$ * should be exchanged by $_{\dagger}$ (and vice versa) in the properties of materials M_2 and M_3 . The symbols * and \dagger indicate the diffusion coefficients that are required to be similar. An alternative approach to design and calculate the anisotropic properties of the multilayer shells is included in Supporting Information.

From an experimental perspective, the realization of the proposed structures should take advantage of the recent advances in the manufacture of multilayer systems at the nanoscale, which offer an avenue for the experimental realization of the systems. $^{32-36}$ We also note that multilayer composites are one alternative to achieve anisotropic systems but other routes, which are also consistent with the proposed theoretical development, include the use of oriented nonspherical inclusions in a matrix material. 37 The use of intrinsically anisotropic materials, if available, constitutes an additional experimental route. We also note that the particular design shown in Figure 2b should not be confused with a multistage process. Our devices use a single pressure difference ($P_{\text{HIGH}} - P_{\text{LOW}}$), in contrast to multistage systems,

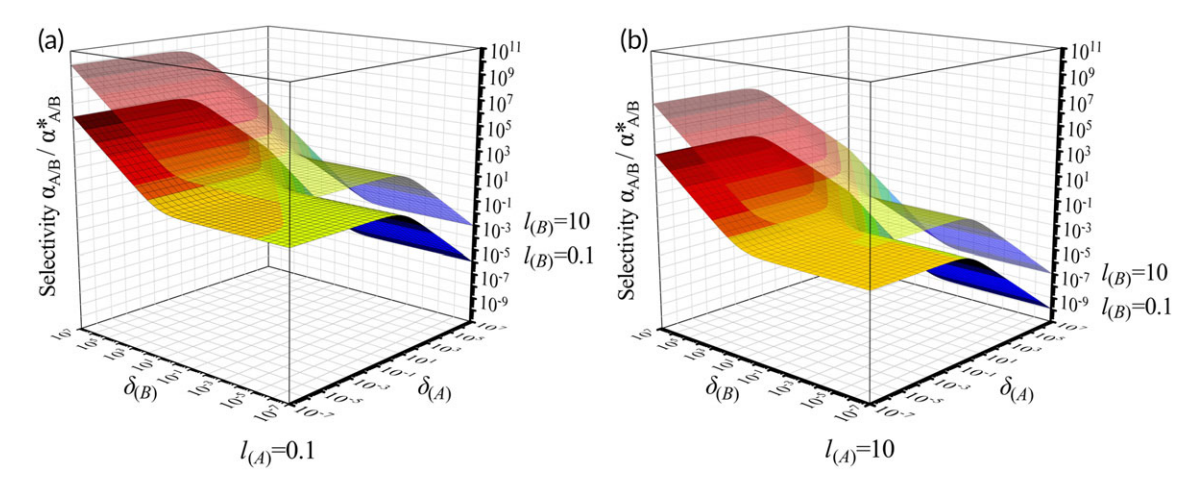


FIGURE 3 Normalized selectivity as a function of the nondimensional variables $I_{(i)}$ and $\delta_{(i)}$ for a shell/core ratio $R_2/R_1 = 2$. (a) $I_A = 0.1$, (b) $I_A = 10$

where a set of pressure differences (one at each stage) is employed. We also stress that the proposed theoretical development applies to all the structures in Figure 2 and more generally to any anisotropic shell (i.e., beyond layered materials as in Figure 2b). In addition, the spatial dependence of the flux magnitude on the permeate side allows us to collect the permeate fraction of interest in a region that maximizes the selectivity or permeance of the device, which is in contrast to isotropic systems, where all the permeate that leaves the membrane is typically collected. Clearly, by collecting a fraction of the permeate in our devices there is an implicit trade-off between purity and recovery.

We calculate in Figures 3 and 4 the performance of the proposed anisotropic membranes in terms of the normalized selectivity and permeance as a function of the design variables $l_{(A)}$, $l_{(B)}$, $\delta_{(A)}$, and $\delta_{(B)}$ for an aspect ratio $R_2/R_1=2$. Figure 3a,b present the relative selectivity $\alpha_{A/B}/\alpha_{A/B}^*$ measuring the increase (or decrease) of the membrane selectivity with respect to the selectivity of the isotropic core without the shell. From the plots it can be seen how, for a fixed value of $\delta_{(A)}$ and $\delta_{(B)}$ the selectivity for A increases when $l_{(A)}$ decreases and $l_{(B)}$

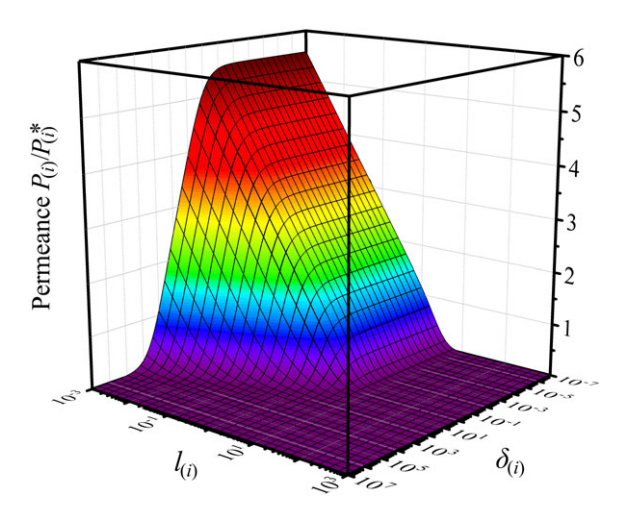


FIGURE 4 Normalized permeance as a function of $l_{(i)}$ and $\delta_{(i)}$ for a ratio R_2/R_1 = 2

increases. This increase in selectivity can be explained by considering that a higher $\alpha_{A/B}$ is obtained when molecules of A are focused toward the core and molecules of B are detoured around it. In other words, to improve the performance it is necessary to favor the transport of A in the radial direction with respect to the azimuthal direction (i.e., small $I_{(A)}$) and simultaneously hinder the radial transport of B (i.e., large $I_{(B)}$). In terms of the structure of the shell, this means that the membranes shown in Figure 2a offer the best performance. Note that in the opposite case when $I_{(A)} > 1$, $I_{(B)} < 1$, the anisotropic shell favors the transport of B toward the core instead of A, this results in an inversion of the selectivity, such that B instead of A is collected at the core of the device (Figures 2d and 3c). Note that the performance is characterized under ideal conditions where boundary conditions are constant in space and time, assuming perfect mixing in the fluid, and neglecting concentration polarization. The shielding effect created when the magnitude of l_i is increased can also be observed in Figure 4, where we plot the normalized permeance $P_{(i)}/P_{(i)}^*$ as a function $I_{(i)}$ and $\delta_{(i)}$. It can be seen from the plot that for a fixed value of $\delta_{(i)}$ the normalized permeance of i from the core decreases as $I_{(i)}$ increases, which corresponds to a stronger shielding shell. Note that the selectivity increases when permeance of A is high ($I_{(A)}$ small) and the permeance of B is low $(I_{(B)} | \text{large}).$

The performance of the system is also determined by the values of the nondimensional variables $\delta_{(A)}$, and $\delta_{(B)}$. We can see from Figure 4 that for a constant value of $I_{(i)}$ the normalized permeance of i increases when the value of $\delta_{(i)}$ decreases. Therefore $\alpha_{A/B}/\alpha_{A/B}^*$ should increase for small $\delta_{(A)}$ (large permeance of A) and large $\delta_{(B)}$ (small permeance of B), which agrees with the selectivity plots shown in Figure 3. This behavior can also be analyzed by considering a fixed core material ($D_{c(i)}$ and $S_{c(i)}$ are constant) and noting that in order to make $\delta_{(A)}$ small (such that normalized permeance of A increases) it is required to increase the intrinsic permeance $\sqrt{D_{sh(A)\theta}D_{sh(A)r}}S_{sh(A)}$ of the anisotropic shell, thus causing an increase in the amount of compound A that enters the shell and therefore the permeance at the core $P_{(A)}/P_{(A)}^*$. Analogously, to obtain a large $\delta_{(B)}$, we need to reduce the

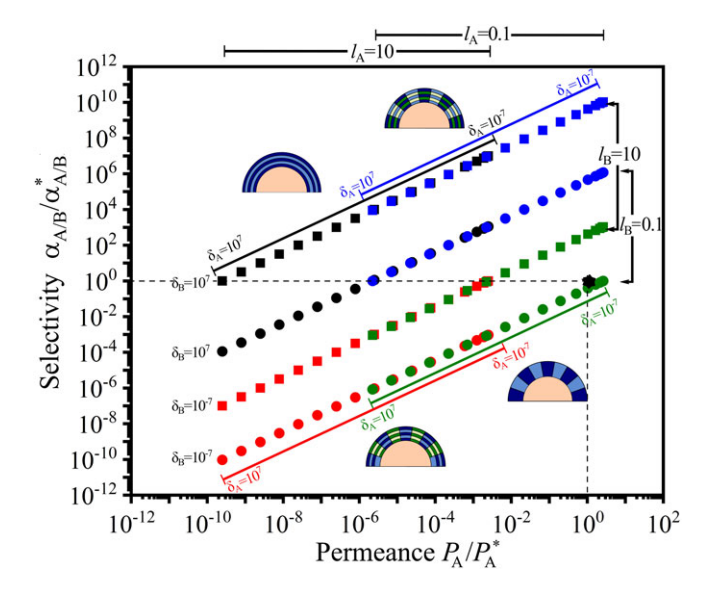


FIGURE 5 Selectivity versus permeance for different values of the nondimensional variables $\delta_{(A)}$, $\delta_{(B)}$, $l_{(A)}$, and $l_{(B)}$

shell permeance for B. This reduction causes a smaller amount of compound B to enter the shell and in the limiting case the normalized permeance tends to zero at the core, in agreement with the trend observed in Figure 4.

In Figure 5, we plot the normalized selectivity versus permeance of our proposed membranes. For reference, we show with a black star the selectivity and permeance of the core material, which corresponds to $\alpha_{A/B}/\alpha_{A/B}^*=1$ and $P_{(A)}/P_{(A)}^*=1$. We can see how different values of selectivities and permeances can be obtained for different values of the nondimensional variables $I_{(A)}$, $I_{(B)}$, $\delta_{(A)}$, $\delta_{(B)}$. Figure 5 shows that the

selectivity and permeance of this system can be broadly manipulated through the structural design of the shell. Note that in many cases, higher selectivity values are achieved in the case of the anisotropic membrane. We note that the feasible region in Figure 5 depends on the mix to be separated and needs to be established for each gas pair based on the properties of the available materials for that specific mix. It is also interesting to note that under certain conditions similar performances can be achieved with different structures. For example, black and blue squares in Figure 5 represent membranes with $I_{(B)}$ =10 and $\delta_{(B)}$ =10.7. The black squares have $I_{(A)}$ =10 while the blue squares have $I_{(A)}$ =0.1 and the performance is modulated by $\delta_{(A)}$. Note that there exist overlapping regions where similar performances can be achieved by using different structures.

To provide insight on the dynamics of anisotropic mass separation membranes, we show in Figure 6 the concentrations profiles (color maps where red corresponds to high concentration and blue to low concentration) and flux lines (white arrows) for compounds A and B within the membrane for the systems shown in Figure 2a,d. The concentration profiles were obtained using finite-element software COMSOL Multyphysics®. On the upper panels, we consider membranes made of homogeneous anisotropic materials, while in the lower panels, we consider the corresponding layered membranes made of isotropic materials, which are obtained via effective medium theory (Equations 9–12). The imposed boundary conditions are $p_i = 1$ atm at the upper boundary and $p_i = 0$ atm at the bottom of the structures. The plots clearly show the functionalities of the structures, since it can be seen in Figure 6 how compounds A and B are focused toward the core or shielded from the core depending on the values of $I_{(A)}$ and $I_{(B)}$. For simplicity, we assume constant solubility across the

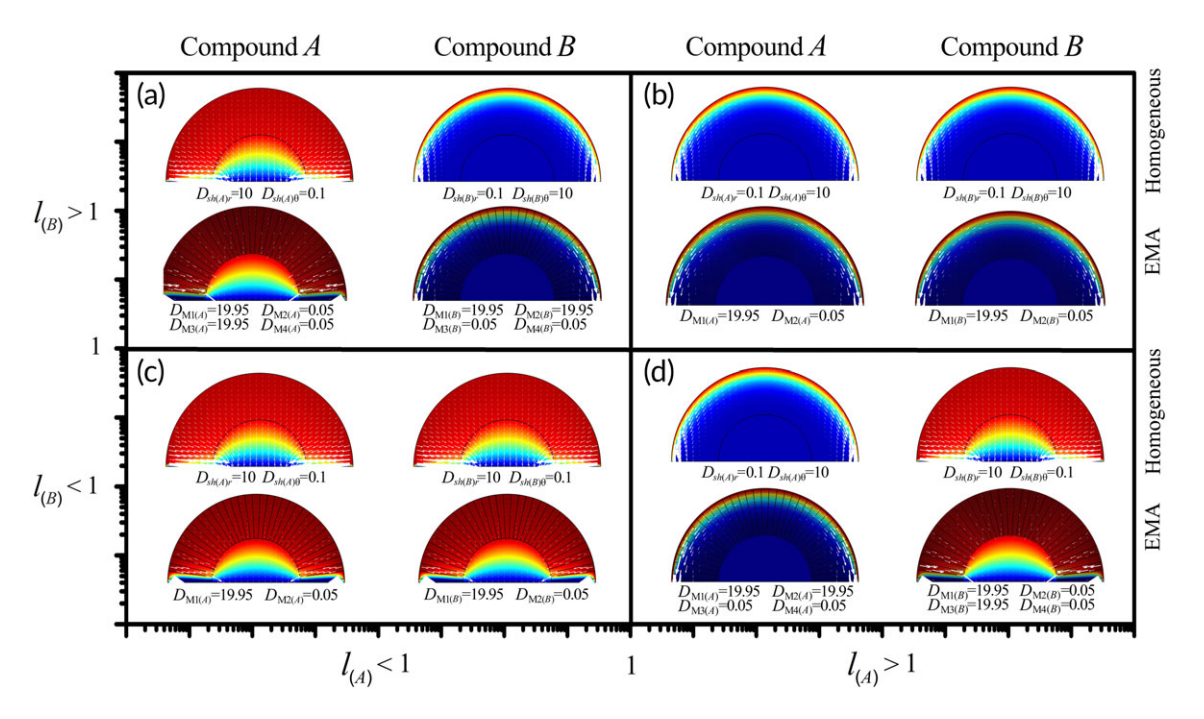


FIGURE 6 Color maps for concentration distribution of compounds A (left) and B (right) inside the anisotropic membranes. We show both homogeneous anisotropic shells (top) and the corresponding multilayer shells (bottom) obtained by effective medium theory (a) $I_A < 1$, $I_B > 1$ (b) $I_A > 1$, $I_B > 1$ (c) $I_A < 1$, $I_B < 1$ (d) $I_A > 1$, $I_B < 1$. For simplicity, the materials are assumed to have similar solubilities

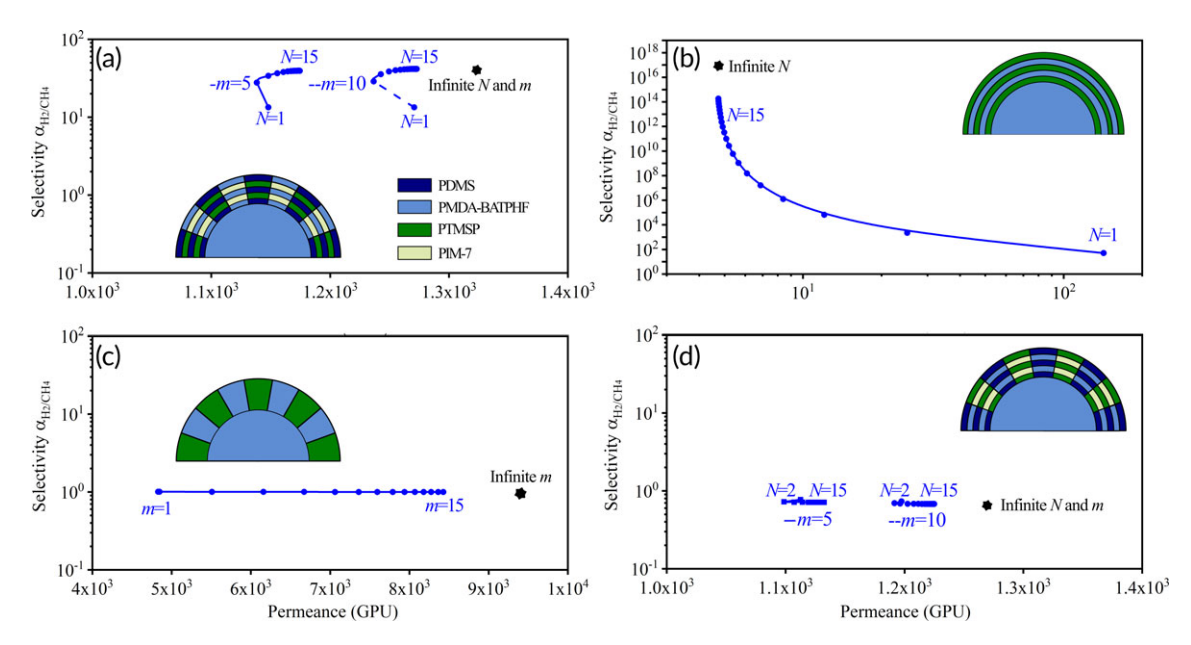


FIGURE 7 Selectivity versus permeance for different anisotropic membranes for separation of H_2/CH_4 with different number of azimuthal N and radial m layers (blue circles) (a) CH_4 shielded from the core and H_2 focused toward the core. (b) Both CH_4 and H_2 are shielded from the core. (c) Both CH_4 and H_2 are focused toward the core. (d) CH_4 is focused toward the core and CH_2 is shielded from the core. The black stars correspond to homogeneous anisotropic shells. Results are presented for CH_4 and CH_4 is shielded from the core.

constituent materials. Importantly, we can see that the flux trajectories followed by compounds A and B in the homogeneous anisotropic material and the effective multilayer composite are similar showing that the layered structures can reproduce the required anisotropy to redirect the flux of A and B. Clearly, this similarity asymptotically increase with increasing number of layers per unit volume.^{28,38}

We next apply our proposed approach to a realistic system and introduce anisotropic membranes for separation of the binary system $\rm H_2/CH_4$. This binary mixture was selected due to its relevance in the recovery of hydrogen.⁶ We found four isotropic materials PTMSP,³⁹ PDMS,⁴⁰ PIM-7,⁴¹ and PMDA-BATPHF⁴² which allow to obtain the shell structures with the different anisotropies for $\rm H_2$ and $\rm CH_4$ as shown in Figure 7. These materials have been selected such that the effective properties of the resulting composites satisfy the constraints in terms of the magnitude of $\it I_A$ and $\it I_B$ in each of the shells (e.g., in Figure 7b $\it I_A$ > 1 and $\it I_B$ > 1). The physical properties of the materials

are listed in Table 1 (additional results for PSF⁴³ and PDMS are presented in Supporting Information). We show in Figure 7 our numerical predictions for selectivity $\alpha_{\rm H_2/CH_4}$ versus permeance $P_{\rm H_2}$ for the different types of membranes as a function of the number of buildingblocks. In Figure 7b we plot α versus P (blue lines) for membranes with increasing number of bilayers N arranged in the azimuthal direction while in Figure 7c the membranes have increasing number of bilayers m arranged in the radial direction. On the other hand, the membranes in Figure 7a,d are described in terms of the total number of bilayers N and m in the azimuthal and radial directions respectively. For reference, we also show the selectivity and permeance values when the shells are made of a homogeneous anisotropic material (black stars), which corresponds to the limiting case of a large number of bilayers N and m. We note that the performance of the multilayer membranes approaches that of a homogeneous anisotropic system when the number of bilayers N and m increases. In terms of performance for

TABLE 1 Diffusion properties of the shell materials in Figure 7

	S _(H2) (mol/m ³ Pa)	D _(H2) (m ² /s)	S _(CH4) (mol/m ³ Pa)	D _(CH4) (m ² /s)	$D_{sh(H2)r}$ (m ² /s)	$D_{sh(H2)\theta}$ (m ² /s)	$D_{sh(CH4)r}$ (m ² /s)	$D_{sh(CH4)\theta}$ (m ² /s)
PTMSP	1.74×10^{-4}	2.60×10^{-8}	1.25×10^{-3}	3.60×10^{-9}				
PDMS	2.41×10^{-4}	1.10×10^{-9}	3.62×10^{-3}	5.10×10^{-12}				
PIM-7	1.98×10^{-5}	1.29×10^{-8}	1.67×10^{-4}	2.17×10^{-9}				
PMDA-BATPHF	6.94×10^{-5}	2.20×10^{-10}	4.22×10^{-4}	6.90×10^{-13}				
Shell Figures 2a-7a	1.26×10^{-4}		1.40×10^{-3}		2.10×10^{-9}	2.03×10^{-9}	1.37×10^{-11}	2.45×10^{-10}
Shell Figures 2b-7b	1.22×10^{-4}		8.36×10^{-4}		2.50×10^{-10}	1.86×10^{-8}	6.95×10^{-13}	2.69×10^{-9}
Shell Figures 2c-7c	1.22×10^{-4}		8.36×10^{-4}		1.86×10^{-8}	2.50×10^{-10}	2.69×10^{-9}	6.95×10^{-13}
Shell Figures 2d-7d	1.26×10^{-4}		1.40×10^{-3}		2.03×10^{-9}	2.10×10^{-9}	2.45×10^{-10}	1.37×10^{-11}

The effective properties for the shells are calculated using effective medium theory (Supporting Information).

hydrogen separation, the membranes shown in Figure 7a offer both large selectivities and permeances. On the other hand, the membranes in Figure 7b,c show very high selectivities and low permeances (Figure 7b) and high permeances and low selectivities (Figure 7c). Interestingly, in Figure 7d we obtain a selectivity inversion where the membranes become CH_4 selective. Importantly, this selectivity inversion is achieved by only changing the arrangement of isotropic materials, thus changing the effective medium properties, and not by chemical modifications of the constituent materials. The above results show the rich behavior in terms of selectivities and permeances that can be obtained by considering anisotropic mass diffusion membranes for separation.

3 | CONCLUSIONS

In this work we studied a new type of membrane materials for gas separations. These novel membranes are achieved by tailoring anisotropic material properties for mass diffusion in order to manipulate the trajectory of the diffusing molecules. This is in contrast to conventional chemical modifications of membrane materials for separations, which only modify the flux magnitude. The required anisotropicity for mass diffusion is obtained in practice by considering composite materials and using effective medium approaches to design their effective anisotropic properties. As shown in our article, anisotropic membranes can have an important impact on the separation performance since manipulation of mass diffusion via anisotropic materials provides new mechanisms to perform membrane gas separations.

ACKNOWLEDGMENTS

This work is supported by the National Science Foundation [Grant No. 1744212].

NOTATION

concentration of species i
concentration of species i in the core
concentration of species i in the shell
diffusivity tensor of species i
diffusion coefficient of species i in the core
Azimuthal diffusion coefficient of species \emph{i} in
the shell
radial diffusion coefficient of species \emph{i} in the
shell
diffusion coefficient of species \emph{i} in materials
$M_1, M_2, M_3, \text{ and } M_4$
$\ \text{effective shell diffusion coefficient for materials} $
connected in parallel
$\ \text{effective shell diffusion coefficient for materials} \\$
connected in series
material volume fraction
flux of species i

$K_{(i)}$	partition coefficient between the core and the
	shell for species i
k_i^*	partition coefficient between two constituent
•	shell materials
$I_{(i)}^2$	ratio of azimuthal to radial diffusion coefficient
W)	for species i
m	number of bilayers arranged in the radial direc-
	tion in the shell
N	number of bilayers arranged in the azimuthal
	direction in the shell
p_i	partial pressure of species i
$P_{(i)}$	permeance of species i for anisotropic device
$P_{(i)}^*$	permeance of species i for isotropic core
R_1	radius of the core
R_2	external radius of the shell
$S_{c(i)}$	solubility of species i in the core
$S_{sh(i)}$	solubility of species i in the shell
$S_{1(i)}, S_{2(i)}, S_{3(i)}, S_{4(i)}$	solubility of species i in materials M_1 , M_2 , M_3 ,
	and M_4
$lpha_{A/B}$	selectivity of the anisotropic device
$lpha_{A/B}^*$	selectivity of the core material

ORCID

 $\delta_{(i)}$

Juan-Manuel Restrepo-Flórez https://orcid.org/0000-0001-5944-8502

core/shell material permeability ratio

Martin Maldovan Dhttps://orcid.org/0000-0002-6256-8465

REFERENCES

- Sholl DS, Lively RP. Seven chemical separations to change the world. Nature. 2016;532(4):435-437.
- Oak Ridge National Laboratory. Materials for separation technologies: energy and emission reduction opportunities. Oak Ridge: Oak Ridge National Laboratory; 2005.
- Sanders DF, Smith ZP, Guo R, et al. Energy-efficient polymeric gas separation membranes for a sustainable future: a review. *Polymer*. 2013;54(18):4729-4761.
- Baker RW, Low BT. Gas separation membrane materials: a perspective. Macromolecules. 2014;47(20):6999-7013.
- 5. Baker RW. Future directions of membrane gas separation technology. *Ind Eng Chem Res.* 2002;41(6):1393-1411.
- 6. Bernardo P, Drioli E, Golemme G. Membrane gas separation: a review/state of the art. *Ind Eng Chem Res.* 2009;48(10):4638-4663.
- Koros WJ, Coleman MR, Walker DRB. Controlled permeability polymer membranes. Annu Rev Mater Sci. 1992;22:47-89.
- 8. Jue ML, Lively RP. Targeted gas separations through polymer membrane functionalization. *React Funct Polym*. 2015;86:40-43.
- Robeson LM. The upper bound revisited. J Memb Sci. 2008;320(1-2): 390-400.
- Koros WJ, Fleming GK. Membrane-based gas separation. J Memb Sci. 1993;83:1-80.
- 11. Koros WJ, Zhang C. Materials for next-generation molecularly selective synthetic membranes. *Nat Mater.* 2017;16(3):289-297.
- Robeson LM. Correlation of separation factor versus permeability for polymeric membranes. J Memb Sci. 1991;62(2):165-185.

- 13. Wijmans JG, Baker RW. The solution-diffusion model: a review. *J Memb Sci.* 1995:107(1–2):1-21.
- gwi KW, Nair S. Membranes from nanoporous 1D and 2D materials: a review of opportunities, developments, and challenges. *Chem Eng Sci.* 2013;104:908-924.
- Shah M, McCarthy MC, Sachdeva S, Lee AK, Jeong HK. Current status of metal-organic framework membranes for gas separations: promises and challenges. *Ind Eng Chem Res.* 2012;51(5):2179-2199.
- Singh A, Koros WJ. Significance of entropic selectivity for advanced gas separation membranes. *Ind Eng Chem Res.* 1996;35 (4):1231-1234.
- Park HB, Kamcev J, Robeson LM, Elimelech M, Freeman BD. Maximizing the right stuff: the trade-off between membrane permeability and selectivity. Science. 2017;356:eab0530.
- Zimmerman CM, Singh A, Koros WJ. Tailoring mixed matrix composite membranes for gas separations. J Memb Sci. 1997;137(1-2):145-154.
- Robeson LM. Polymer blends in membrane transport processes. Ind Eng Chem Res. 2010;49(23):11859-11865.
- Vu DQ, Koros WJ, Miller SJ. Mixed matrix membranes using carbon molecular sieves I preparation and experimental results. J Memb Sci. 2003;211(2):311-334.
- 21. Mahajan R, Burns R, Schaeffer M, Koros WJ. Challenges in forming successful mixed matrix membranes with rigid polymeric materials. J Appl Polym Sci. 2002;86(4):881-890.
- Chung TS, Jiang LY, Li Y, Kulprathipanja S. Mixed matrix membranes (MMMs) comprising organic polymers with dispersed inorganic fillers for gas separation. *Prog Polym Sci.* 2007;32(4):483-507.
- Restrepo-Flórez JM, Maldovan M. Mass separation by metamaterials. Sci Rep. 2016;6(2):21971.
- Restrepo-Flórez J-M, Maldovan M. Metamaterial membranes. J Phys D Appl Phys. 2017:50:25104.
- Guenneau S, Puvirajesinghe TM. Fick's second law transformed: one path to cloaking in mass diffusion. J R Soc Interface. 2013;10(83): 20130106.
- Guenneau S, Petiteau D, Zerrad M, Amra C, Puvirajesinghe T. Transformed Fourier and Fick equations for the control of heat and mass diffusion. AIP Adv. 2015;5(5):053404.
- Zeng L, Song R. Controlling chloride ions diffusion in concrete. Sci Rep. 2013:3:3359.
- Restrepo-Flórez J-M, Maldovan M. Breaking separation limits in membrane tehnology. J Memb Sci. 2018;566:301-306.
- Restrepo-Flórez JM, Maldovan M. Mass diffusion cloaking and focusing with metamaterials. Appl Phys Lett. 2017;111(7):071903.
- 30. Davis HT. The effective medium theory of diffusion in composite media. *J am Ceram Soc.* 1977;60(11–12):499-501.
- 31. Sax J, Ottino JM. Modeling of transport of small molecules in polymer blends: application of effective medium theory. *Polym Eng Sci.* 1983; 23(11):165-176.

- 32. Borges J, Mano JF. Molecular interactions driving the layer-by-layer assembly of multilayers. *Chem Rev.* 2014;114(18):8883-8942.
- 33. Richardson JJ, Björnmalm M, Caruso F. Technology-driven layer-by-layer assembly of nanofilms. *Science* (80-). 2015;348(6233):aaa2491.
- 34. Ajitha AR, Aswathi MK, H.J. M, Izdebska J, Thomas S. In: Kim J, Thomas S, Saha P, eds. *Multicomponent polymeric materials*. Vol 223. Dordrecht: Springer; 2016.
- Ponting M, Hiltner A, Baer E. Polymer nanostructures by forced assembly: process, structure, and properties. *Macromol Symp.* 2010; 294(1):19-32.
- Gupta M, Lin Y, Deans T, Baer E, Hiltner A, Schiraldi DA. Structure and gas barrier properties of poly (propylene-graft-maleic anhydride)/ phosphate glass composites prepared by microlayer coextrusion. *Macromolecules*. 2010;43:4230-4239.
- Moccia M, Castaldi G, Savo S, Sato Y, Galdi V. Independent manipulation of heat and electrical current via bifunctional metamaterials. *Phys Rev X*. 2014;4(2):021025.
- Restrepo-Flórez JM, Maldovan M. Rational design of mass diffusion metamaterial concentrators based on coordinate transformations. J Appl Phys. 2016;120(8):084902.
- Merkel TC, Bondar V, Nagai K, Freeman BD. Perfluorocarbon gases in poly (1-trimethylsilyl-1-propyne). J Polym Sci Part B Polym Phys. 2000; 38:273-296.
- Merkel TC, Bondar VI, Nagai K, Freeman BD, Pinnau I. Gas sorption, diffusion, and permeation in poly(dimethylsiloxane). J Polym Sci Part B Polym Phys. 2000;38(3):415-434.
- Budd PM, Msayib KJ, Tattershall CE, et al. Gas separation membranes from polymers of intrinsic microporosity. *J Memb Sci.* 2005;251(1-2): 263-269.
- Tanaka K, Kita H, Okano M, Okamoto K. Permeability and permselectivity of gases in fluorinated and non-fluorinated polyimides. *Polymer*. 1992;33(3):585-592.
- McHattie JS, Koros WJ, Paul DR. Gas transport properties of polysulfones: 1. Role of symmetry of methyl group placement on bisphenol. *Polymer*. 1991;32(5):840-850.

SUPPORTING INFORMATION

Additional supporting information may be found online in the Supporting Information section at the end of this article.

How to cite this article: Restrepo-Flórez J-M, Maldovan M. Anisotropic membrane materials for gas separations. *AIChE J.* 2019;e16599. https://doi.org/10.1002/aic.16599